Dynamics of Spin-Stabilized Spacecraft During Deployment of Telescoping Appendages

R. Sellappan* and P. M. Bainum†
Howard University, Washington, D. C.

The dynamics of a spin-stabilized spacecraft with telescoping appendages are treated analytically and numerically. Two types of telescoping appendages are considered: a) where the end masses are mounted at the end of the (assumed) massless booms and b) where the appendages are assumed to consist of a uniformly distributed homogeneous mass throughout their lengths. For the telescoping system, Eulerian equations of motion are developed. During all deployment sequences, it is assumed that the transverse component of angular momentum is much smaller than the component along the major spin axis. Closed-form analytical solutions for the time response of the transverse components of angular velocity are obtained for the spacecraft hub having a spherical and nearly spherical mass distribution. For the more general case, a series solution is obtained and this solution is limited by its radius of convergence. A comparison of the different approximate analytical methods with numerical integration results is provided. From these results it is seen that the oscillatory nature of the responses of the transverse angular velocity components reduces rapidly with faster extension rates.

Nomenclature

$a_1(t), a_2(t)$	= time varying coefficients in the approximate equations for $\dot{h}_2, \dot{h}_1$, respectively
A_n	= coefficients in the series solution for $h_1(t)$
$b(t)$	= time varying coefficient in the exact equations for $\dot{h}_1$ and $\dot{h}_2$
c	= boom extension rate
h_1, h_2, h_3	= components of the angular momentum vector along the principal axes
h_0	= assumed constant value of h_3 during nominal deployment maneuver
I_1, I_2, I_3	= instantaneous values of principal moments of inertia
I_1^*, I_2^*, I_3^*	= hub principal moments of inertia
I^*	= moment of inertia of the spherical spacecraft hub
$\ell(t)$	= instantaneous length of the boom from the center of the spacecraft hub
$\dot{\ell}(t)$	= extension rate of the boom
ℓ_f	= final extension length of the boom
m	= end mass
P	$= 2mc^2$
p	$= (I^*/P)^{1/2}$
q_0	= initial amplitude of the transverse angular momentum
q	$= (3I^*/Q)^{1/3}$
Q	$= 2\rho c^3/3$
R	= radius of convergence of the series solution
t	= time
$\omega_1, \omega_2, \omega_3$	= angular velocities about the 1,2, and 3 axes
ρ	= mass density per unit boom length
Ψ_0	= initial phase angle in the solution for h_1, h_2
Ω	= hub nutation frequency $= \omega_3(0)(I_3^* - I^*)/I^*$
$\cdot$	= indicates time differentiation
(0)	= indicates initial conditions

Received Jan. 15, 1976; presented as Paper 76-185 at the AIAA 14th Aerospace Sciences Meeting, Washington, D. C. Jan. 16-28, 1976; revision received June 3, 1976. This research was supported by NASA Grant No. NGR-09-011-053 (Suppl. No. 1); special appreciation to V. Huff, NASA HQ and to C. W. Martz, W. Anderson, NASA Langley for many helpful discussions.

Index category: Spacecraft Attitude Dynamics and Control

*Graduate Research Assistant, Dept. of Mechanical Engineering. Formerly with Indian Scientific Satellite Project, Bangalore, India. Student Member AIAA.

†Professor of Aerospace Engineering, Dept. of Mechanical Engineering. Associate Fellow AIAA.

Introduction

A NUMBER of spin-stabilized spacecraft have long appendages which nominally lie in the plane of rotation perpendicular to the desired spin axis. These appendages might be onboard antennas which must be extended in orbit after the initial injection sequence. The extension of onboard antenna booms usually is done with the use of motors located in the central hub of the spacecraft.

Of special interest is the stability of the system during the initial extension of boom-type telescoping appendages. An early investigation considers this problem for the case of telescoping-type appendages consisting of two end masses at the ends of massless rods.[1] It is assumed that the extension maneuver is restricted to a plane which is perpendicular to the

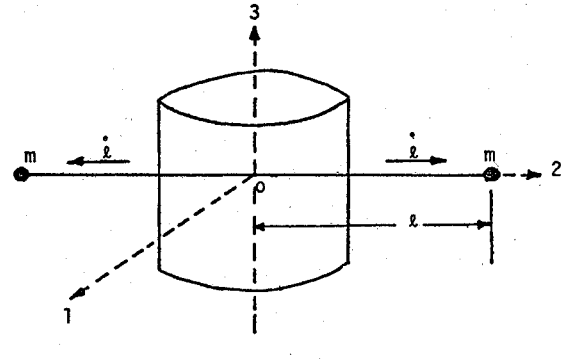

a) Moving end mass system

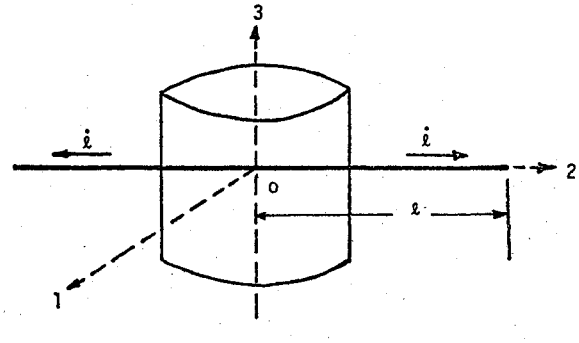

b) Uniformly distributed moving mass system

Fig. 1 Two types of telescoping appendages.

nominal spin axis and that both the system angular momentum and kinetic energy are conserved. In addition, the transverse components of angular velocity are assumed to be zero during extension. Under these assumptions, it is seen that the resulting Lagrange equations of motion will yield an approximate analytical solution for limiting values of initial-to-final moment of inertia ratios.[1] A more recent treatment using an Eulerian formulation considers the extension of rigid booms of uniformly distributed mass where the transverse component of angular momentum remains less than the polar component throughout extension. For the special case where the spin axis is an axis of symmentry, the linearized equations can be solved analytically.[2]

In a recent paper, Bainum and Sellappan[3] considered the application of telescoping appendages to detumble a randomly spinning spacecraft. It was concluded that by controlling the boom extension maneuvers the spacecraft could be brought close to either a zero inertial spin state or a flat spin final state.[3]

The present study will examine the three-dimensional angular motion of a general (asymmetrical) spinning spacecraft having telescoping appendages during initial deployment. For these initial (nominal) deployment operations, in accord with actual practice, it will be assumed that the transverse component of angular momentum is much smaller than the component along the major spin axis. The dynamics of such a system will be studied using a variety of analytical techniques, for special cases, and numerical methods for the general case.

Analysis

A. General Considerations

The motion and stability of spin-stabilized spacecraft with telescoping appendages are studied analytically and numerically. The telescoping appendages considered here are of varying length and could represent extensible antennas or a tether connected to the main part of the spacecraft. Extensions for the telescoping appendages are considered to originate from the center of the spacecraft hub.

The torque-free equations for a spacecraft with varying moments of inertia are

$$\dot{h}_1 = \omega_3 h_2 - \omega_2 h_3, \dot{h}_2 = \omega_1 h_3 - \omega_3 h_1 \dot{h}_3 = \omega_2 h_1 - \omega_1 h_2 \tag{1}$$

where the angular momentum is defined as

$$h_i(t) = I_i(t)\omega_i(t) \tag{2}$$

For the special case of a symmetrical spacecraft hub ($I_1^* = I_2^* = I^*$) and symmetrical extensions of the telescoping appendages along the "1" and "2" axes [spin axis being an axis of symmetry: $I_1(t) = I_2(t) = I(t)$], Eqs. (1), reduce to

$$\dot{h}_1 = -b(t)h_2 \tag{3}$$

$$\dot{h}_2 = b(t)h_1 \tag{4}$$

$$\dot{h}_3 = 0 \tag{5}$$

where

$$b(t) = \{[I_3(t) - I(t)]/[I_3(t)I(t)]\}h_0 \tag{6}$$

$$h_0 = h_3(0) \tag{7}$$

The solutions to Eqs. (3) and (4) can be written as[3]

$$h_1(t) = q_0 \cos\left(\int_0^t b(t)\,dt + \psi_0\right) \tag{8}$$

$$h_2(t) = q_0 \sin\left(\int_0^t b(t)\,dt + \psi_0\right) \tag{9}$$

The solutions given by Eqs. (8) and (9) are identical with those given in Ref. 2 for the same physical conditions.

Next, we consider the extension of the appendages in the "2" axis directions only. The equations for $h_1(t)$ and $h_2(t)$, with the following approximations: $|h_1|$, $|h_2| \ll |h_3|$ and

$$h_3 = h_0 = \text{const.} \tag{10}$$

can be written as

$$\dot{h}_1 = -a_2(t)h_2 \tag{11}$$

$$\dot{h}_2 = a_1(t)h_1 \tag{12}$$

where $a_1(t)$ and $a_2(t)$ are defined as

$$a_1(t) = \{[I_3(t) - I_1(t)]/[I_3(t)I_1(t)]\}h_0 \tag{13}$$

$$a_2(t) = \{[I_3(t) - I_2(t)]/[I_3(t)I_2(t)]\}h_0 \tag{14}$$

For the case where the spacecraft hub is spherical, we note that $I_1(t) = I_3(t)$ and hence from Eq. (13), $a_1(t) \equiv 0$. Thus, Eq. (12) reduces to $\dot{h}_2(t) = 0$, and we obtain

$$h_2(t) = h_2(0) \tag{15}$$

Since I_2 remains constant, $\omega_2(t)$ remains unchanged from its initial value and is given by

$$\omega_2(t) = \omega_2(0) \tag{16}$$

Integration of Eq. (11) results in the time response of the angular momentum h_1 for the particular applications which are considered in the following sections.

Two types of telescoping appendages are considered (Fig. 1): a) the case where the end masses are mounted at the end of the (assumed) massless booms (moving end mass system) and b) where the appendages are assumed to consist of a uniformly distributed, homogeneous mass throughout their lengths (uniformly distributed moving mass system). The case of the moving end mass system is considered in detail, whereas for the case of the uniformly distributed moving mass system the final results are presented.

B. Moving End Mass System

1) Analytical Solution for Spherical Hubs

The telescoping system with each end mass m attached at the end of the (assumed) massless rods which move in the "2" axis directions is shown in Fig. 1a. Extensions for the telescoping system are considered to originate from the center of the spacecraft hub (Fig. 1a).

The moments of inertia about the three principal axes during the extension are (from Fig. 1a)

$$I_1 = I_1^* + Pt^2, \qquad I_2 = I_2^*, \qquad I_3 = I_3^* + Pt^2 \tag{17}$$

where $P = 2mc^2$ and $\ell = ct$, and for this application $I_i^* = I^*$ $(i = 1, 2, 3)$. The equations that are developed in the earlier section for the case of the spacecraft hub being spherical are applied here. Equation (11), after substitution of Eqs. (14, 15, and 17), can be written as

$$\dot{h}_1 = -\left(\frac{h_0 h_2(0)}{I^*}\right)\left(\frac{t^2}{p^2 + t^2}\right) \tag{18}$$

where $p^2 = I^*/P$. Integration of Eq. (18) with respect to time yields

$$h_1(t) = -[h_0 h_2(0)/I^*](t - \Phi) + D \tag{19}$$

where $\Phi = p \tan^{-1}(t/p)$ and D is a constant which is determined from the initial condition for h_1. The final expression for $\omega_1(t)$ is obtained as

$$\omega_1(t) = \frac{\omega_1(0) - \omega_3(0)\omega_2(0)(t-\Phi)}{1+(t^2/p^2)} \tag{20}$$

The time response of $\omega_3(t)$ is obtained from $h_3 = h_0$ as

$$\omega_3(t) = h_0/(I_3^* + Pt^2) \tag{21}$$

Equations (20, 16, and 21) represent the expressions for the time responses of the angular velocities ω_1, ω_2, and ω_3, respectively, of the spacecraft during the extensions of the moving end mass system.

2) Series Solution for Nonspherical Hubs

For the general case of a nonspherical spacecraft hub and extensions in the "2" axis directions, the expressions for the transverse angular velocities represented by Eqs. (20) and (16), respectively, cannot be used as these equations are valid only when the spacecraft hub is spherical. The following approach, for the general case, is taken to obtain independent differential equations for h_1 and h_2. These then are used to develop the series solutions for the transverse angular velocities. Differentiating Eq. (11) with respect to time and using Eq. (12), the resulting equation for h_1 is

$$\ddot{h}_1 - [\dot{a}_2(t)/a_2(t)]\dot{h}_1 + a_1(t)a_2(t)h_1 = 0 \tag{22}$$

Similarly, the equation for h_2 results as

$$\ddot{h}_2 - [\dot{a}_1(t)/a_1(t)]\dot{h}_2 + a_1(t)a_2(t)h_2 = 0 \tag{23}$$

Equations (13, 14, and 17) are used in Eq. (22) to obtain the following second-order ordinary differential equation for h_1:

$$\ddot{h}_1 - \frac{2I_2^* Pt}{(I_3^* + Pt^2)(I_3^* - I_2^* + Pt^2)}\dot{h}_1 + \frac{(I_3^* - I_1^*)(I_3^* - I_2^* + Pt^2)h_0^2}{(I_3^* + Pt^2)^2 (I_1^* + Pt^2) I_2^*} h_1 = 0 \tag{24}$$

The second-order differential equation for h_2 is obtained, in a procedure similar to that used for h_1, as

$$\ddot{h}_2 + \frac{(I_1^* + I_3^* + 2Pt^2)2Pt}{(I_3^* + Pt^2)(I_1^* + Pt^2)}\dot{h}_2 + \frac{(I_3^* - I_1^*)(I_3^* - I_2^* + Pt^2)h_0^2}{(I_3^* + Pt^2)^2 (I_1^* + Pt^2) I_2^*} h_2 = 0 \tag{25}$$

It can be seen that Eqs. (24) and (25) contain time-dependent coefficients with complex regular singular points.

Equations (24) and (25) are used to obtain the series solutions for $h_1(t)$ and $h_2(t)$. A similar type of series solution has been used previously to predict the planar librational motion of a gravity-gradient satellite during boom deployment.[4] Here $t=0$ is an ordinary point of Eqs. (24) and (25) and the radius of convergence R is the smaller value of $[(I_3^* - I_2^*)/P]^{1/2}$ or $(I_1^*/P)^{1/2}$.

The series solution for h_1 may be expanded about $t=0$ in the form

$$h_1 = \sum_{n=0}^{\infty} A_n t^n \tag{26}$$

It can be shown that the odd coefficients can be related to A_1 and the even coefficients to A_0.[5] The solution for $h_1(t)$ is written as

$$h_1(t) = A_0[F_1(t)] + A_1[G_1(t)] \tag{27}$$

where $F_1(t)$ contains the even-powered terms and $G_1(t)$ the odd-powered terms. The constants A_0 and A_1 are determined from the initial conditions as follows:

$$A_0 = h_1(0) = I_1^* \omega_1(0) \tag{28}$$

$$A_1 = \dot{h}_1(0) = I_1^* \dot{\omega}_1(0) \tag{29}$$

The expression for $\omega_1(t)$ is given by

$$\omega_1(t) = [h_1(t)]/[I_1^* + Pt^2] \tag{30}$$

In a similar way, a series solution for $h_2(t)$ can be obtained.[5] The response for $\omega_2(t)$ has the form

$$\omega_2(t) = [h_2(t)]/I_2^* \tag{31}$$

An expression for $\omega_3(t)$ results directly from the idea of conservation of $h_3 (\equiv h_0)$:

$$\omega_3(t) = h_0/(I_3^* + Pt^2) \tag{32}$$

In general, for a symmetrical spacecraft hub, the initial conditions $\dot{\omega}_1(0)$ and $\dot{\omega}_2(0)$ can be related to $\omega_1(0)$ and $\omega_2(0)$ from the torque-free precession before the extension begins. However, it should be noted that such initial angular accelerations also may be caused by other types of external perturbations.

3) Analytical Solution for Nearly Spherical Hubs

When the hub is nonspherical ($I_3^* \neq I^*$), the spacecraft exhibits a nutational motion. For the case where the hub is nearly spherical ($I_1^* = I_2^* \simeq I_3^* = I^*$) we note that $\dot{h}_2(t) \neq 0$ from Eq. (12), and, hence, the angular velocity about the "2" axis is not exactly equal to the initial value.

The solutions for the transverse components of the angular velocity are obtained from Eqs. (24) and (25) by making the approximation: $I_1^* = I_2^* \simeq I_3^* = I^*$. Equations (24) and (25) reduce to

$$\ddot{h}_1 - \frac{2I^*}{(I^* + Pt^2)t}\dot{h}_1 \simeq 0 \tag{33}$$

$$\ddot{h}_2 + \frac{4Pt}{(I^* + Pt^2)}\dot{h}_2 \simeq 0 \tag{34}$$

The solution of Eq. (33) for $\omega_1(t)$ is the same as in Eq. (20). The expression for $\omega_2(t)$ can be obtained from Eq. (34) as

$$\omega_2(t) \simeq \omega_2(0) + \frac{\dot{\omega}_2(0)}{2}\left(\frac{p^2 t}{p^2 + t^2} + \Phi\right) \tag{35}$$

where p and Φ are defined in conjunction with Eqs. (18) and (19), respectively. The initial condition $\dot{\omega}_2(0)$ is related to $\omega_1(0)$ from the torque-free precession before the extension operations start. For $\dot{\omega}_2(0) = 0$, Eq. (35) reduces to Eq. (16), where there is no initial nutation.

C. Uniformly Distributed Moving Mass System

1) Analytical Solution for Spherical Hubs

The telescoping system having a uniformly distributed boom mass (ρ = boom mass/unit length), which moves in the "2" axis directions is shown in Fig. 1b. As before, extensions for this telescoping system are considered to originate from the center of the hub (Fig. 1b).

The moments of inertia during this deployment can be expressed by

$$I_1 = I_1^* + Qt^3, \qquad I_2 = I_2^*, \qquad I_3 = I_3^* + Qt^3 \tag{36}$$

where $Q=2\rho c^3/3$ and $\ell=ct$. From the comparison of Eqs. (17) and (36), it is clear that the equations of motion for the uniformly distributed moving mass system can be obtained from the equations of motion for the moving end mass system by replacing P with Qt. Following the procedure used for the moving end mass system (Sec. B.1), the expressions for $\omega_1(t)$ and $\omega_2(t)$ are obtained for the case of a spherical hub, as,

$$\omega_1(t)=\frac{\omega_1(0)-\omega_3(0)\omega_2(0)(t-\alpha-\beta)}{1+(t^3/q^3)} \tag{37}$$

$$\omega_2(t)=\omega_2(0) \tag{38}$$

where

$$\alpha=\frac{q}{6}\ln\left[\frac{(t+q)^2}{t^2-qt+q^2}\right]$$

$$\beta=\frac{q}{3^{1/2}}\left[\tan^{-1}\left(\frac{2t-q}{3^{1/2}q}\right)+\frac{\pi}{6}\right]$$

$$q^3=3I^*/Q$$

2) Analytical Solution for Nearly Spherical Hubs

A procedure similar to that used in Sec. B.3 is followed. The expression for $\omega_1(t)$ is the same as in Eq. (37), but the solution for $\omega_2(t)$ is obtained as

$$\omega_2(t)\simeq\omega_2(0)+\frac{\dot\omega_2(0)}{3}\left[\frac{q^3t}{q^3+t^3}+2\alpha+\beta\right] \tag{39}$$

where α,β, and q are already defined with reference to Eq. (37).

Numerical Results

In this section the results from numerical integration of the nonlinear differential equations of motion for the most general case are presented and are compared with the approximate analytical results. From the analytical solutions obtained, it is found that the solutions for the cases of spherical and nearly spherical spacecraft hubs are the same when $\dot\omega_2(0)=0$. The case of a nearly spherical hub is considered here for comparison with the results from numerical integration. The system parameters selected are $I_1^*=I_2^*=5.0$ slug-ft^2; $I_3^*=5.05$ slug-ft^2 (nearly spherical hub); $m=0.01$ slug (each end mass); $\rho=0.0042$ slug/ft (boom density); and $\ell_f=60$ ft (final extension length). The assumed initial conditions are $\omega_1(0)=0.075$ rad/sec; $\omega_2(0)=0$; $\omega_3(0)=3.34$ rad/sec.

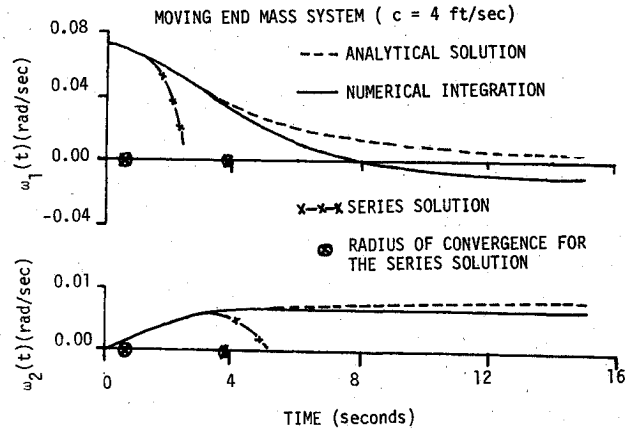

Fig. 2 Comparison of analytical, numerical integration, and series solution results.

The initial angular accelerations, $\dot\omega_1(0)$ and $\dot\omega_2(0)$, are obtained, for a nearly spherical hub, from the torque-free precession as $\dot\omega_1(0)=\Omega\omega_2(0)$ and $\dot\omega_2(0)=\Omega\omega_1(0)=0.0025$ rad/sec^2. The initial angular accelerations, $\dot\omega_1(0)$ and $\dot\omega_2(0)$, are needed only for obtaining the series solutions for $\omega_1(t)$ and $\omega_2(t)$, and the analytical solution, $\omega_2(t)$, when the spacecraft hub is nearly spherical.

A. Moving End Mass

A typical time response of the components of transverse angular velocity for a nearly spherical hub is shown in Fig. 2 and 3. End mass extension rates of $c=4$ and $c=3$ ft/sec, respectively, are considered where extension is assumed to occur only along the "2" axis. For numerical integration Eqs. (1) and (17) are used to obtain the results. The analytical solutions, given by Eqs. (20) and (35) and the series solution, given by Eqs. (30) and (31), with ten terms present, are compared with the numerical integrations. It is observed that the analytical solution corresponds more closely with the numerical results as the extension rate is increased. The series

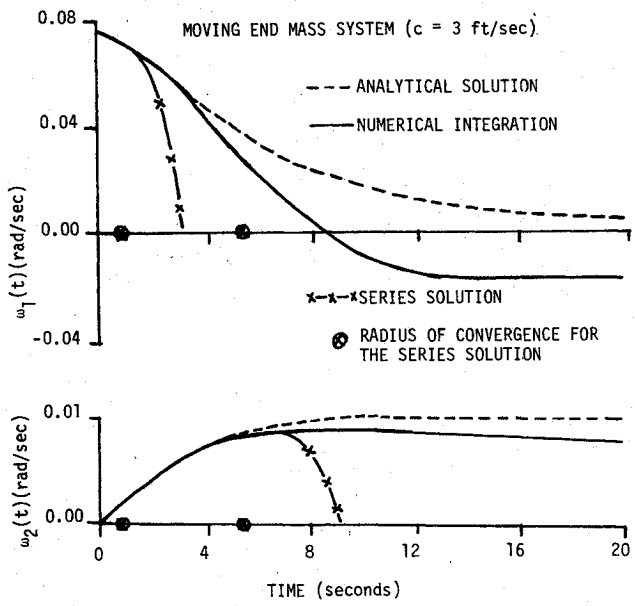

Fig. 3 Comparison of analytical, numerical integration, and series solution results.

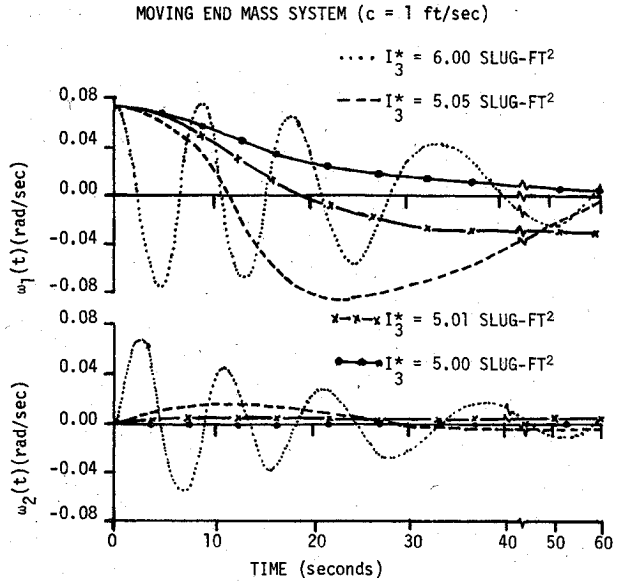

Fig. 4 Effect of varying the hub spin axis moment of inertia (numerical integration).

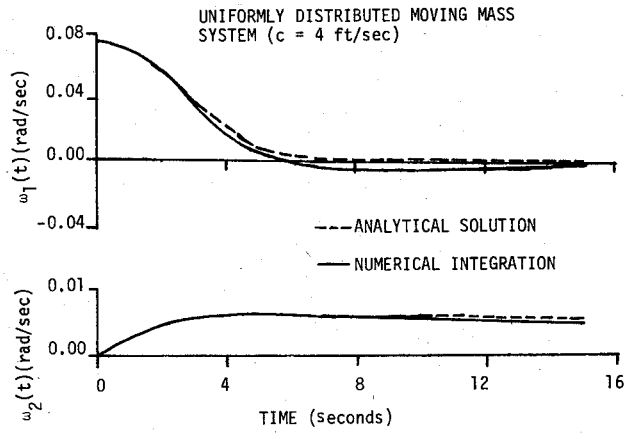

Fig. 5 Comparison of analytical and numerical integration results.

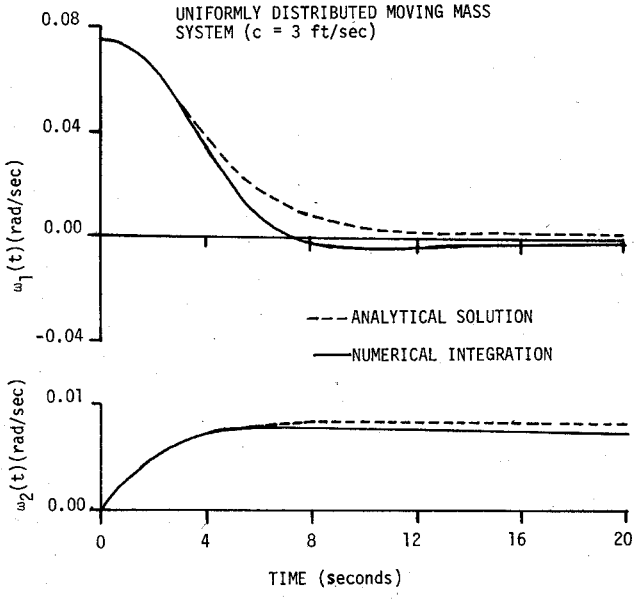

Fig. 6 Comparison of analytical and numerical integration results.

solution can be used only in the initial part of the extension where the analytical solution gives essentially the same result. The series solution is limited by its radius of convergence as shown for each case.

In Fig. 4, the effect of varying the hub spin axis moment of inertia is shown using numerical integration. It is observed that when the hub spin axis moment of inertia (I_3^*) is increased from the spherical case ($I_3^*=I_1^*=I_2^*=5$ slug-ft^2), the transverse angular responses tend to become more oscillatory over the full deployment time. For the case when $I_3^*=6$ slug-ft^2, $I_1^*=I_2^*=5$ slug-ft^2, a series solution also was investigated, but its limited radius of convergence made it unhelpful for this application.

B. Uniformly Distributed Moving Mass System

Figures 5 and 6 represent a typical comparison of analytical with numerical integration results. Extension rates $c=4$ and 3 ft/sec, respectively, are assumed for a symmetrical deployment of the extensible members, but only along the "2" axis. The approximate analytical results, obtained from Eqs. (37) and (39) are compared with the numerical integration of Eqs. (1) using the moments of inertia given in Eq. (36). It is observed that the analytical solution gives an excellent correlation with the numerical integration for the higher extension rate, whereas for the lower extension rate, the accuracy is slightly diminished. (The same type of improvement with faster deployment has been noted previously

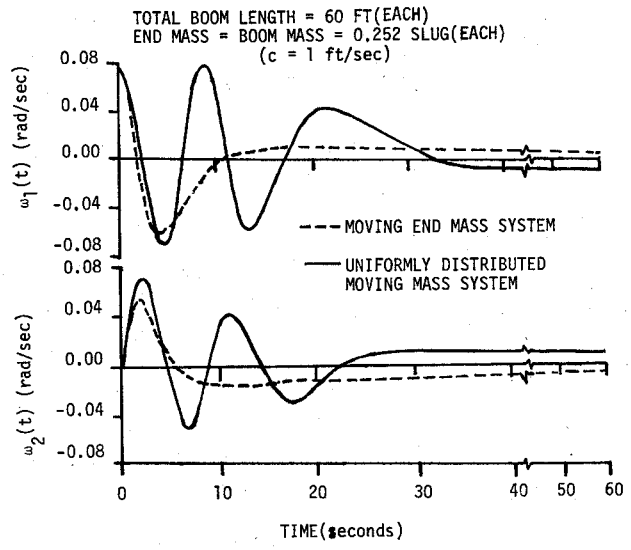

Fig. 7 Comparison of performance of both types of telescoping systems (numerical integration).

for the case of the end mass moving system, Fig. 2). Because of the very limited radius of convergence for the series solution, a comparison with this method of solution was not performed for the case of uniformly distributed mass booms.

The response of both types of telescoping systems, considering the uniformly distributed mass replaced by an equivalent end mass, is shown in Fig. 7. It is seen that, initially, both types yield approximately the same responses; however, the amplitudes of the transverse angular velocities are rapidly reduced for the end mass moving system. This shows the effect of an increased moment of inertia, as time increases, because of the total mass being located at the end of the boom.

Additional numerical results, for both types of telescoping systems and for different extension rates and end masses have been obtained. These are presented in Ref. 5.

Conclusions

As a result of the present analysis and the corresponding numerical results, the following conclusions were reached.

1) For both types of telescoping systems, closed-form analytical solutions, for the transverse components of angular velocity as functions of time, were obtained for the special case where the spacecraft hub (main part) has a nearly spherical mass distribution, and, where the telescoping system is assumed to deploy from the hub mass center along one of the transverse axis directions only.

2) It is observed that the analytical solution corresponds more closely with the numerical integration results as the extension rate is increased. The series solution can be used only in the initial part of the extension because of convergence constraints, but here the analytical solution gives essentially the same results. It is to be noted that the analytical solution gives an excellent correlation with the numerical integration at the higher extension rates for the uniformly distributed mass system.

3) In the general case, the numerical integration results show that the oscillatory nature of the transverse angular velocity components is reduced rapidly at the larger extension rates.

References

[1]Lang, W. and Honeycutt, G. H., "Simulation of Deployment Dynamics of Spinning Spacecraft," NASA-TN-D-4074, Aug. 1967.

[2]Huges, P. C., "Dynamics of a Spin-Stabilized Satellite During Extension of Rigid Booms," *CASI Transactions*, Vol. 5, March 1972, pp. 11-14.

[3]Bainum, P. M. and Sellappan, R., "Spacecraft Detumbling Using Movable Telescoping Appendages," *26th Congress of the International Astronautical Federation,* Paper No. 75-113, Sept. 21-27, 1975, Lisbon, Portugal; to be published in *Acta Astronautica.*

[4]Puri, V. and Bainum, P. M., "Planar Librational Motion of a Gravity-Gradient Satellite During Deployment," *Astronautical Research 1971,* D. Reidel Publishing Co., Dordrecht, Holland, 1973, pp. 63-80.

[5]Bainum, P. M. and Sellappan, R., "The Dynamics of Spin Stabilized Spacecraft with Movable Appendages," Pt. I, Final Rept., NASA Grant NGR-09-011-053 (Suppl. No. 1), May 1975, Howard Univ., Dept. of Mechanical Engineering, Washington, D.C.